

# A comparative study between self-piercing riveting and resistance spot welding of aluminium sheets for the automotive industry

L. Han<sup>1,a\*</sup>, M. Thornton<sup>1,b</sup>, M. Shergold<sup>2,c</sup>

1, Warwick Manufacturing Group, University of Warwick, Coventry, CV4 7AL, UK,  
a, [li.han@warwick.ac.uk](mailto:li.han@warwick.ac.uk), b, [martin.thornton@warwick.ac.uk](mailto:martin.thornton@warwick.ac.uk), c, [mshergo1@jaguarlandrover.com](mailto:mshergo1@jaguarlandrover.com)

\*Corresponding author: Tel: +44(0)2476575385; Fax: +44(0)24767575366

**Abstract:** The increased application of lightweight materials, such as aluminium has initiated many investigations into new joining techniques for aluminium alloys. The Resistance Spot Welding (RSW) concept for aluminium has always attracted many researchers from different organizations. Self-piercing riveting (SPR) is the major production process used to join aluminium sheet body structures for the automotive industry. The research team at the University Of Warwick has investigated these two major joining technologies for aluminium assembly. The paper reported here gives an in depth comparison of the mechanical behavior for each joint type under different loading conditions. It covers symmetrical and asymmetrical assembly from thin gauge of 1.0mm to thick gauge of 3.0mm. The results suggest that generally RSW can provide similar strength performance to SPR with the exception of T-peel; the energy to maximum load needs be considered ‘case to case’ and is dependent largely on loading conditions and the failure mode particularly with respect to SPR. The spread of results for SPR is generally smaller than RSW, and the performance of SPR joints improves as the thickness increases.

**Key words:** (D) Mechanical fastening, (D) Welding, (A) Aluminium sheets

## 1. Introduction

Today’s automotive industry is a challenging business. It is required not only to respond to environmental concerns such as greenhouse gases and fuel economy, but also to meet customer expectations. Therefore, a need for weight reduction has emerged and this in turn has led to the increased application of lightweight materials, such as aluminium and polymer composites. The use of aluminium alloys offers an opportunity for vehicle weight reduction, which can lead to a reduction of fuel consumption and emissions without compromising performance, comfort and safety [1, 2, 3]. Aluminium alloys can offer high corrosion resistance, good formability and good crashworthiness. In addition, the recyclability of aluminium alloys is also a considerable attraction to manufacturers. However, the use of aluminium requires not only a different approach in car design but also a different approach to manufacturing technology and in particular joining methods. As a result many investigations into advanced joining techniques for aluminium structures have been instigated.

Resistance Spot Welding (RSW) of steel is the most popular conventional joining technique for body structures in the automotive industry, but the technology requires adoption of significant process changes in order for it to be suitable for resistance spot welding of aluminium. It is generally recognised that the short life of the welding electrodes and the associated reduction in weld quality as the electrodes degrade [4, 5, 6] present major challenges when welding aluminium. The work previously undertaken by the University of Warwick [7, 8] has proved that significant improvements in electrode life and consequently weld quality can be achieved by rigorous process control. Therefore RSW of aluminium can be a viable volume manufacturing technology.

Self-piercing riveting (SPR) is a key production process used to join aluminium sheet body structures in the automotive industry. The technology has many advantages, such as no pre-drilled hole requirement, capability to join a wide range of similar or dissimilar materials and combinations of materials, no fume emissions etc. However, the process is limited by the inability to change process parameters such as rivet size or die configuration "on the fly" between successive joint positions on a vehicle structure. This leads to potential increasing costs and limits the application of the technology. In addition, the use of steel rivets not only adds weight and cost to Body in White (BIW) assembly, but also raises concerns of recyclability and corrosion. Although SPR offers a practical solution to the automotive industry for joining aluminium alloys, researchers are striving to identify alternative joining process that may avoid some of these issues or reduce costs.

Both SPR and RSW technologies for aluminium assembly and their mechanical properties have been investigated and compared by many researchers and institutes. Lapensee [9] reported that compared with RSW, the static strength of SPR was higher in the case of aluminium to aluminium. However, Razmjoo et al. [10] indicated that the static strength of self-piercing riveted joints was lower than that of resistance spot-welded joints for both steel to steel and aluminium to aluminium joints. It was also observed that the static strength of spot-welded joints was at least 30% higher in aluminium specimens compared with self-piercing riveted joints for identical combinations. Miller et al [11] also reported that the spot welded joint of aluminium AA5754 is the strongest among the SPR and adhesive joining methods studied in both the static and dynamic cases. Additionally, both Riches [12] and Westgate [13] predicted that a high static strength could be achieved for self-piercing riveted joints through a suitable rivet and die design. To date, there remains some contradiction in the public domain regarding the mechanical behavior of RSW and SPR. As the research team at the University of Warwick has recently proved that RSW of aluminium can be a viable volume manufacturing technology [8], it is necessary to have a fresh look at the mechanical behavior of the two joining processes. The paper reported here represents a summary of this research. It aims to compare the static behavior of SPR and RSW joints and covers symmetrical and asymmetrical assembly from thin gauge of 1.0mm to thick gauge of 3.0mm. Static strength and energy absorption data at maximum load for each joint type were compared under different loading conditions. This paper aims to offer design and manufacturing engineers a better insight into the two processes through the back-to-back comparison.

## 2. Experimental procedure

As a key objective of this research is to provide engineering solutions, the materials, stacks and process parameters have been chosen to represent production applications.

### 2.1. Materials

Commercial aluminium alloy AA5754 with various thicknesses was used to form different joint stacks. The automotive grade AA5754-O material was supplied by Novelis and was joined in the as-received pre-treated and lubricated condition. The material properties of the AA5754 aluminium are listed in Table 1.

**Table 1: Compositions and mechanical properties of AA5754 alloy**

MECHANICAL PROPERTIES				
Young's Modulus (GPa)	Tensile strength (MPa)	Elongation	Hardness (H <sub>V</sub> )	
70	240	22%	63.5	
NOMINAL COMPOSITION(BALANCE Al) wt%				
Si	Fe	Cu	Mn	Mg
0-0.40	0-0.40	0-0.10	0-0.50	2.60-3.60

### 2.2. Specimens and test conditions

Industry standard lap shear, T-peel and X-tension samples were made using the two joining processes. To allow for the shunting effect in the resistance spot welding process, lap shear and T-peel samples were produced in large coupons using special fixtures. The final test pieces, with dimensions as shown in Figures 1(a), 1(b) (LE is grip distance), were cut from these large coupons. X-tension samples, shown in Figure 1(c), were produced using a purpose designed lattice fixture to compensate for shunting. For self-piercing riveting, all test pieces were made individually to the same dimensions as shown in Figure 1. At least 5 samples for each process and condition were tested, using a standard Instron tensile test machine with a 30kN load capacity. All tests were carried out using a cross head speed of 10mm/min.

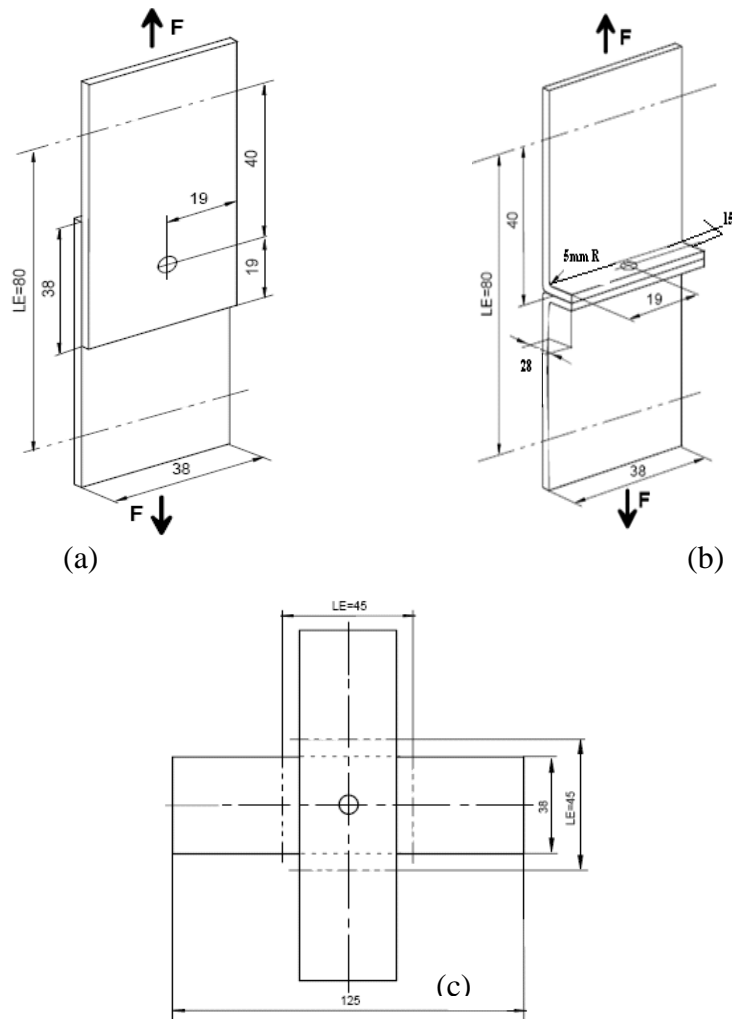


**Figure 1: Samples geometry and dimensions: (a) Lap shear, (b) T-peel, (c) Cross tension (not in scale, LE= Grip distance)**

### 2.3. Process parameter selections

As various rivet and die combinations can be used to produce an SPR joint for a given stack-up, different combinations including one set that was considered to be an optimum selection were chosen. Similar to SPR joints, the nugget size of a RSW joint can range from an industry standard minimum criteria of  $4\sqrt{t}$  (shown in Figures as  $4RT$ ), where  $t$  is the thinnest sheet thickness in the joint stack, to an optimum nugget diameter depending on process parameters. In order to make a fair comparison RSW joints with different nugget diameters were also produced, with one selected to be near to optimum nugget diameter for the stack being tested. Table 2 gives the whole range of stacks and parameter selections. For RSW, nugget diameter was used to indicate different process selections; while for SPR, a Set Number was used to represent different rivet and die combinations for each stack.

**Table 2: Material stacks and Process selections**

Process	Material Stacks						
	1+1	1+2	2+1	2+2	2+3	3+2	3+3
RSW	4√t, 5√t, 6√t,	4√t,	4√t,	4√t, 5√t,	4√t, 5√t,	4√t,	4√t,
SPR	Set 1	Set 1	Set 1	Set 1, 2	Set 1, 2	Set 1	Set 1, 2

### 3. Results and Discussion

#### 3.1. Symmetrical stacks – strength comparison

Figure 2 shows the lap shear, X-tension and T-peel test results for the (1+1) material stack. There were three groups of RSW joints, each having a different nugget diameter from (4√t) to (6√t). These have been compared with a single set of SPR joints made using parameters that represent the optimum settings for this stack. As can be seen from Figure 2, the three groups of RSW joints exhibited different strength values. These show a direct correlation between increasing nugget diameter and strength. For RSW groups above (4√t) nugget diameter, lap shear strengths can exceed those achieved for the optimum SPR joints. The X-tension results showed a similar trend of increasing strength with nugget diameter for (4√t) and (5√t) groups, and the strengths were higher than for the SPR joints. The results for the (6√t) X-tension joints in comparison were unexpectedly low. This may be explained by the increased sensitivity of the X-tension test to peripheral defects, such as weld expulsion that is likely to occur at the higher currents required to achieve a 6√t nugget diameter. In contrast to the lap shear and X-tension test geometries, the highest strength in T-peel was obtained from the SPR samples.

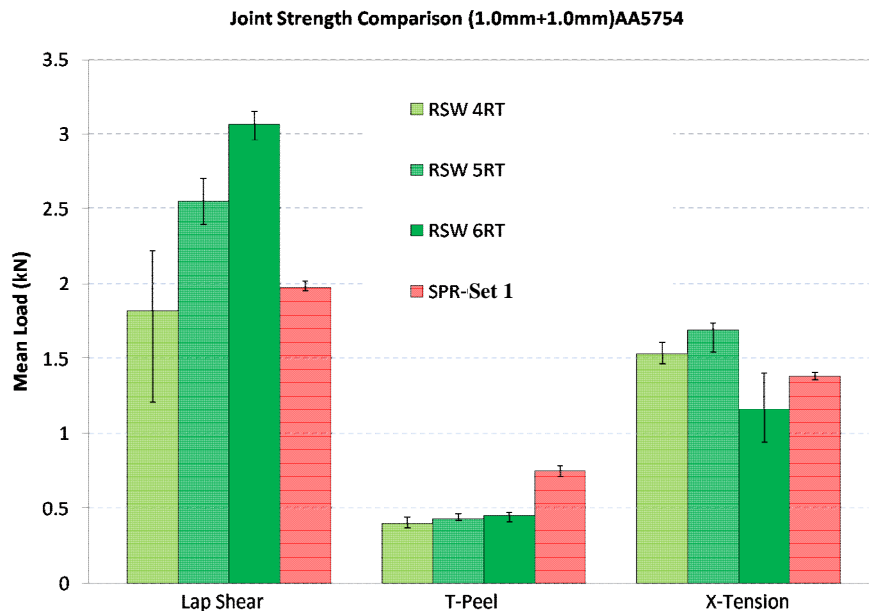


**Figure 2: Joint strength comparison for (1+1) stack**

Figure 3 shows the lap shear, X-tension and T-peel test results for the (2+2) material stack. There were two groups of RSW joints tested; 4√t and 5√t nugget diameter, and two sets of SPR samples having different rivet and die combinations for comparison. For lap shear and X-tension tests, the strength for

RSW joints increased with nugget diameter. RSW joints with  $5\sqrt{t}$  nugget diameter had slightly lower shear strength but exhibited higher X-tension strength than both sets of SPR samples. For T-peel strength, the SPR and RSW  $5\sqrt{t}$  groups were closely matched.

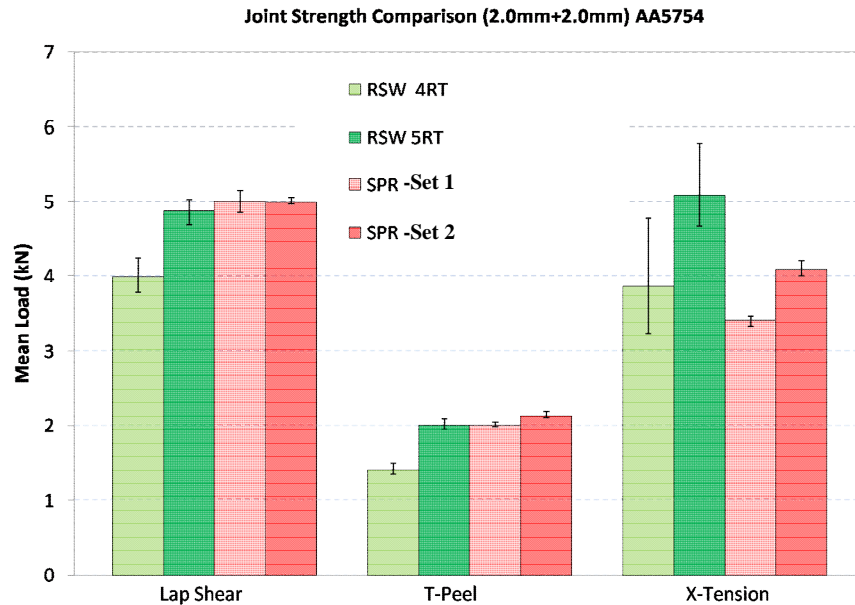


**Figure 3: Joint strength comparison for (2+2) stack**

Figure 4 shows the lap shear, X-tension and T-peel test results for the (3+3) material stack. For this comparison there were two sets of SPR samples with different rivet and die combinations, but only one group of RSW joints with  $4\sqrt{t}$  nugget diameter. The different SPR joint strengths obtained showed the effect of varying the rivet and die combination. Higher strengths could be obtained for SPR in both lap shear and T-peel joint configurations with the optimum rivet and die combination. For X-tension, the joint strength obtained for SPR (optimum rivet and die) and RSW samples were much closer, but the RSW results showed greater scatter.

Some general observations are that for the three symmetrical stacks tested:

- The SPR samples exhibited less scatter than the RSW joints for all test geometries.
- As the thickness increased the SPR samples tended to perform better than the RSW samples.
- The RSW joints showed a correlation between the nugget diameter and strength value in particular for lap shear and X-tension test.

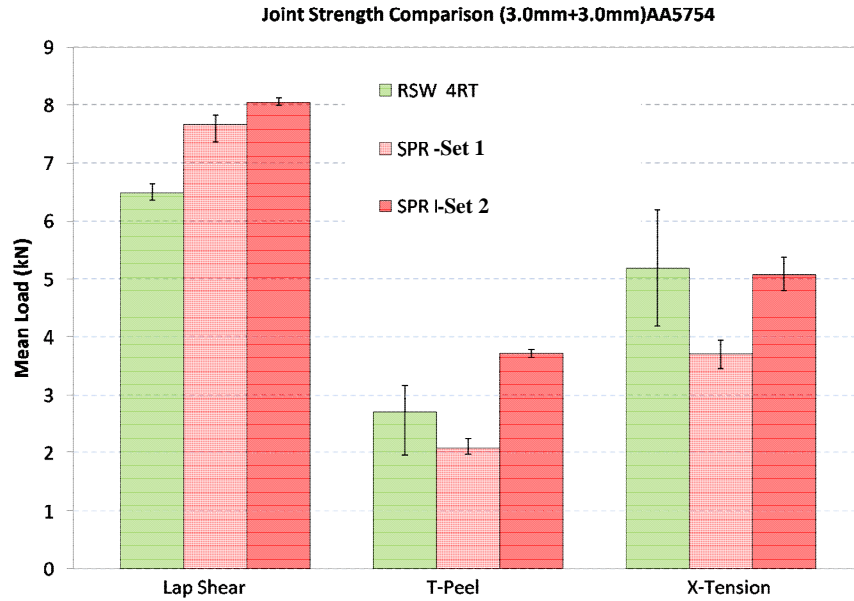


**Figure 4: Joint strength comparison for (3+3) stack**

### 3.2. Symmetrical stacks – analysis of lap shear results

For a lap shear joint, the shear strength is governed by several factors, such as material tensile strength, tearing strength, secondary bending, and specimen configuration, etc [14]. The key influential factor can generally be discovered by examining the failure mode of the specimen. Figure 5 shows the failure modes that occurred for the (1+1) SPR and RSW lap shear samples tested as an example.

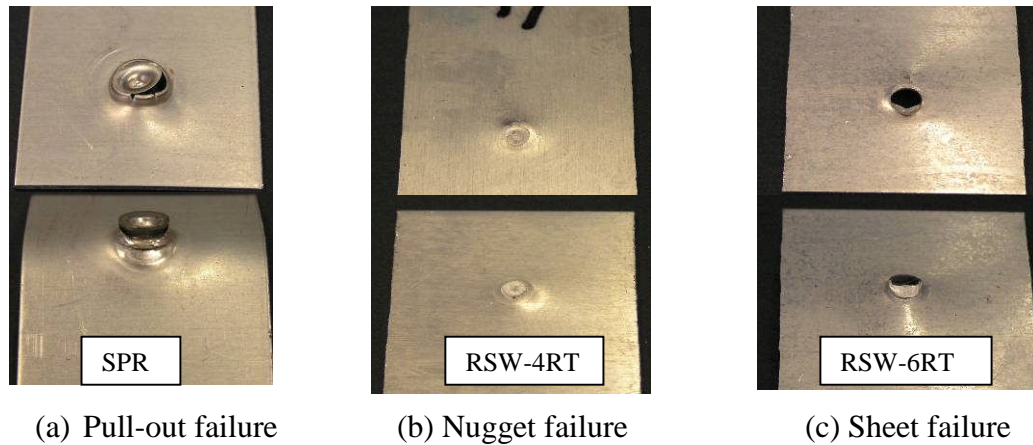


**Figure 5: Failure modes occurred during lap shear test for (1+1) stack**

For SPR, all three symmetrical stacks tested failed with the same mode, which was by the rivet pull out from the bottom sheet, as shown in Figure 5(a). In this situation, it is the interlock between the rivet and the bottom sheet that determines the joint strength. Depending on the rivet and die combination, it can generally be assumed that the greater the interlock - the higher the joint strength. The different sets of SPR samples in these tests had different interlock qualities leading to different strengths.

Two different failure modes were observed for the (1+1) RSW stacks, as shown in Figures 5(b) and (c). For the ( $4\sqrt{t}$ ) samples, nugget failure was observed; whilst sheet pull-out failure occurred for the ( $5\sqrt{t}$ ) and ( $6\sqrt{t}$ ) samples. This is attributed to the formation of the nuggets. Since the ( $4\sqrt{t}$ ) samples were made using a lower current than the ( $5\sqrt{t}$ ) and ( $6\sqrt{t}$ ) samples, it is expected that the samples with smaller nugget diameter should have less nugget penetration than the bigger nugget diameter samples. This was confirmed by micro sections taken of the samples and is shown by the ( $4\sqrt{t}$ ) and ( $6\sqrt{t}$ ) examples in Figure 6.

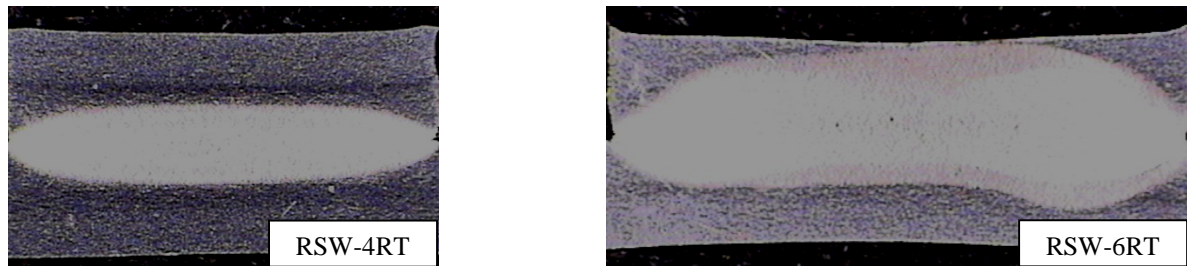


**Figure 6: Sections of RSW samples for (1+1) stack**

During testing the smaller nuggets failed to sustain the shear load, leading to interfacial / nugget failure of the welds. The larger nuggets, which are in closer proximity to the surface, leave a much thinner layer of parent sheet and under shear loading this failed to sustain the load. Therefore a plug containing the undamaged weld was pulled out of the parent sheet. The results suggest that the failure mode and the shear strength for RSW joints depend on formation of the joint, which is related to process parameters. In an ideal situation, the nugget strength should be balanced with the sheet pull-out strength. In reality, this is difficult to control as over penetration of a nugget would cause damage to the electrode surface, which consequently will affect weld quality. For (2+2) and (3+3) stacks, only nugget failure was observed. This is because the remaining parent sheet material is thick enough to sustain higher load than the weld nugget, leading to nugget/interfacial failure of the joints.

### 3.3. Symmetrical stacks – analysis of T-peel results

The SPR joints generally achieved higher or similar T-peel strengths than the RSW samples in the three symmetrical stacks tested. This is attributed to the interlock feature of an SPR type joint. In these tests two different failure modes were observed. Rivet pull-out failure, as shown in the example Figure 7(a), occurred when the rivet interlocked into the bottom sheet was pulled out during the test. This type of failure indicates that the interlock dominates the joint strength. All (1+1) samples failed by the rivet pull-out indicating a weak interlock. For the thicker gauge stacks, there is more material present and it is easier to obtain a good interlock strength, which can exceed the tearing resistance of the parent sheet. Consequently, the failure mode can change to sheet pull out as the head of the rivet is pulled through the sheet. This failure mode was observed for some rivet and die combinations for (2+2) and (3+3) stacks, as shown in Figure 7(b). For RSW samples failure occurred as the sheet material was peeled away along the Heat affected zone (HAZ) leaving a plug of material containing the untouched nugget, as shown in Figure 7(c). This failure mode suggests that the RSW T-peel strength is governed by the tearing resistance of the sheet material (providing the nugget is sufficient strong to sustain the load or else shear/interfacial failure occurs). Although the peel strength increased with nugget diameter, the increment was not as significant as that seen for shear strength.



For both RSW and SPR technologies: the T-peel joint geometry combined with peel loading provides the lowest strength performance of the three geometries tested.

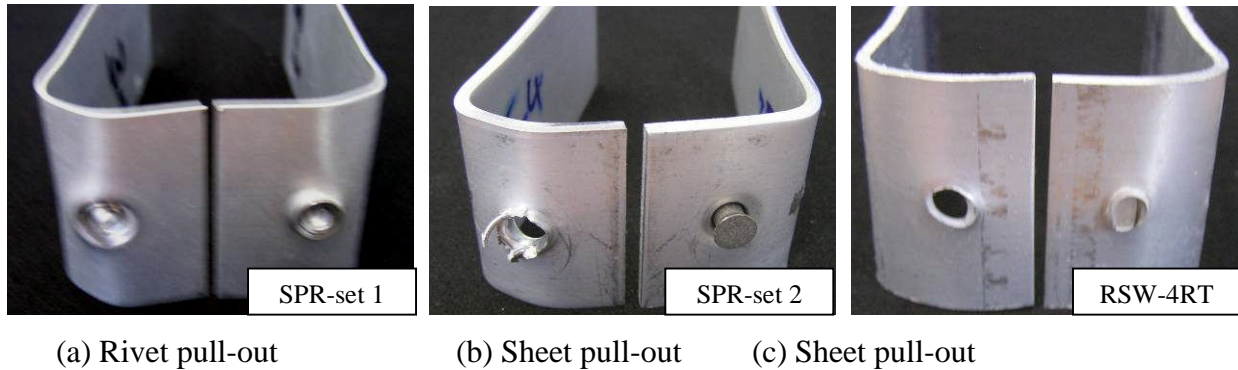


**Figure 7: Failure modes occurred during T-peel test – (2+2) stack**

**3.4. Symmetrical stacks – analysis of X-tension results**

The RSW joint strengths generally matched or exceeded those for the SPR samples in the X-tension test. Even the RSW (3+3) joints made at  $(4\sqrt{t})$  nugget diameter achieved equivalent X-tension strength to the optimum SPR joint stack. In this test geometry, all SPR samples failed by rivet pull-out of the bottom layer, as shown in Figure 8(a); whilst all RSW samples failed by nugget pull-out of the sheet, as shown in Figure 8(b). The failure modes observed indicate that for the X-tension geometry, the interlock of SPR joints is primarily tested, and for RSW samples, the periphery of the weld nugget is important. It follows that the bigger the interlock the higher the X-tension strength for SPR joints, and the bigger the nugget the higher the X-tension strength for RSW samples. Therefore, the joints strengths obtained are highly dependent upon the process parameters chosen, as seen for the other test geometries.

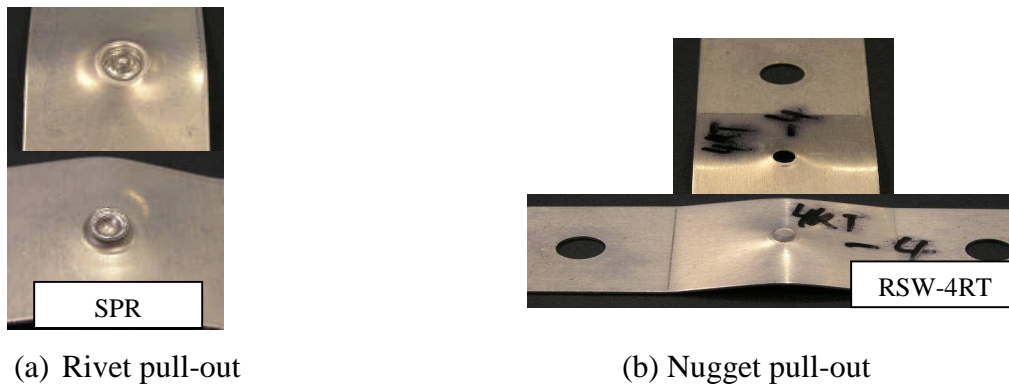


**Figure 8: Failure modes occurred during cross tension test - (1+1) stack**

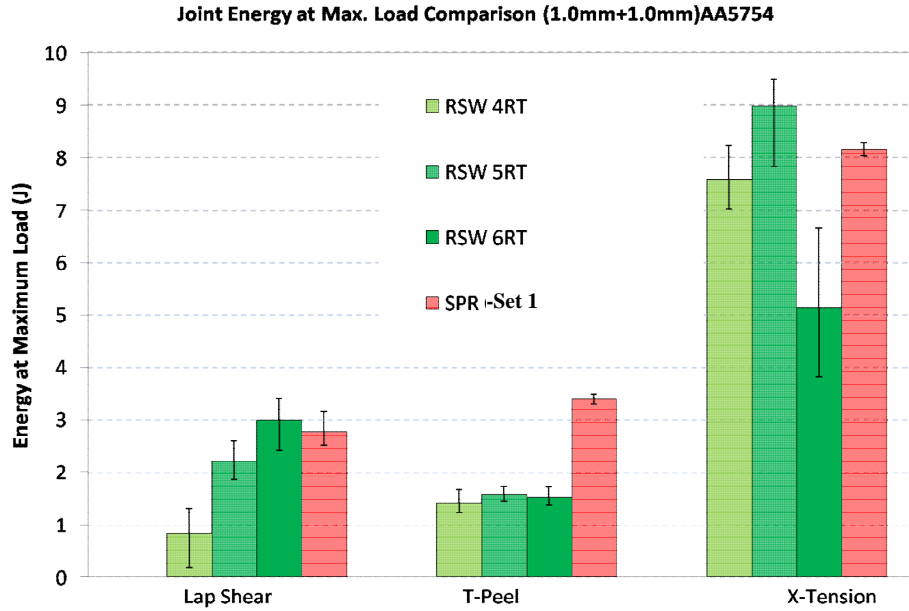
Although both T-peel and X-tension tests exhibited similar final failure mode, the failure process was different. For the T-peel geometry, the sheet material was peeled off the nugget from an initiation point and then along the nugget circumference; whilst for the X-tension test, the sheet had to be pulled away from the complete nugget circumference. Therefore in general, the X-tension strength is greater than the T-peel strength for RSW samples. As the nugget pull-out resistance increases with nugget diameter the RSW joints can have greater X-tension strength than the SPR joints, whose X-tension strength

purely relies on their interlock. These results suggest that depending on loading condition, the strength comparison between SPR and RSW can be changed.

For all three symmetrical stacks, the variation of the strength for SPR joints under all loading conditions was very small indicating a high degree of process consistency; whilst for RSW samples there was more variation in the strength values obtained. This is attributed to differences in nugget diameter, which generally results from variation in surface condition. RSW aluminium is a surface critical process and consequently any local changes in the distribution of the AA5754 surface pretreatment or solid wax lubricant, can affect contact resistances. This is in agreement with previous research on RSW aluminium [15-18]. Although the welding parameters used have been developed to normalise these surface conditions, it is inevitable that some variation in contact resistance could still occur and lead to variation in the strength values. In some cases, the variation can be amplified by using too high current. For example, the RSW samples with  $(6\sqrt{t})$  nugget diameter for (1+1) stack had lower X-tension strength than the joints with  $(4\sqrt{t})$  nugget diameter. The result can be explained as the parameters required to achieve a  $(6\sqrt{t})$  nugget diameter are close to the process boundary conditions, this resulted in two out of five samples expelling leading to a greater variation in the strength value.

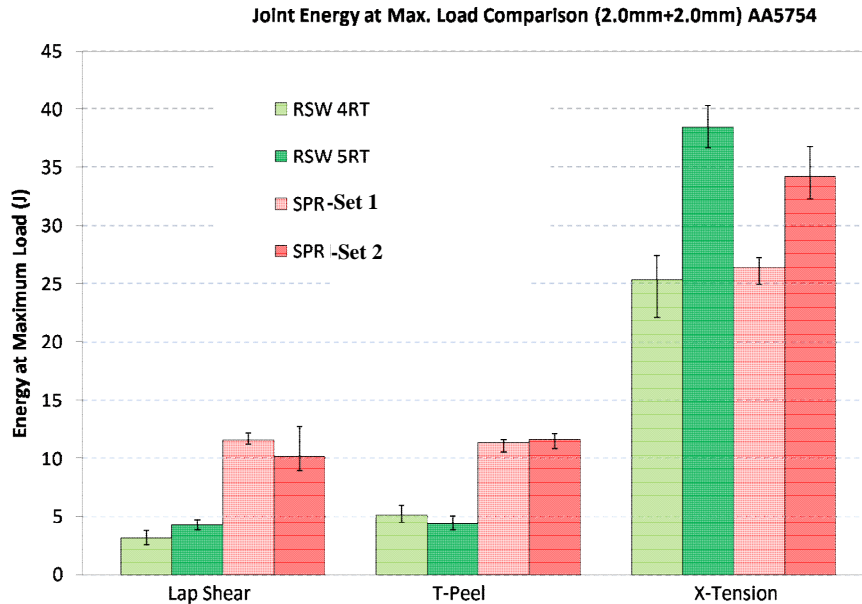
### 3.5. Symmetrical stacks – Energy absorption comparison

Figure 9 shows energy absorption results for the (1+1) RSW and SPR samples at maximum load for each test geometry. The RSW samples with  $(5\sqrt{t})$  nugget diameter exhibited slightly higher energy absorption than the SPR samples under shear loading; whilst the SPR samples showed much higher energy absorption than the RSW samples under peel conditions. Under X-tension loading, the RSW samples with  $(5\sqrt{t})$  nugget diameter achieved higher energy absorption than the SPR samples; but with  $(6\sqrt{t})$  nugget diameter showed much lower values and more scattered data. The use of boundary condition to achieve  $(6\sqrt{t})$  nugget diameter not only resulted in low strength, but also low energy absorption with great variations. The selection of process parameters for the RSW samples had a significant effect on energy absorption results. Depending on loading condition, the RSW samples could exceed the energy absorption at maximum load for (1+1) SPR joint stacks.



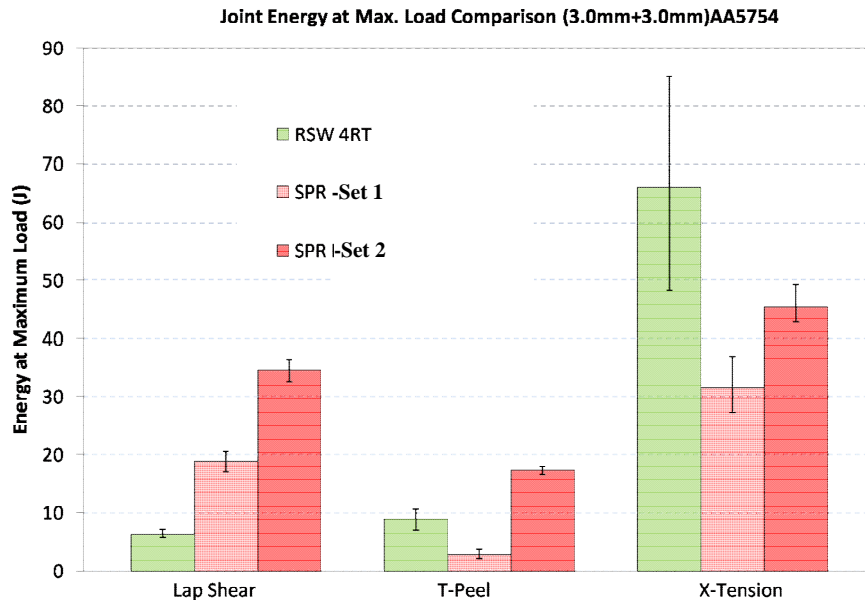
**Figure 9: Energy absorption data at maximum load for SPR and RSW samples – (1+1) stack**

Figure 10 shows energy absorption results for (2+2) stacks. Under shear and peel loadings, both sets of SPR samples achieved much higher values than the RSW samples; whilst under X-tension, the RSW samples with 5√t nugget diameter obtained higher data than both sets of SPR joints. These results indicate that the selection of process parameters for both RSW and SPR joints affect their energy absorption behaviour. Comparing these results with the data shown in Figure 9, it is suggested that even under the same loading condition, different material stacks with different process parameters can lead to a different ranking of the energy absorption data.



**Figure 10: Energy absorption data at maximum load for SPR and RSW samples – (2+2) stack**

Figure 11 shows energy absorption results for (3+3) stacks. Both sets of SPR samples had much higher energy absorption than the RSW joints under shear loading, and one set of the SPR joints achieved higher results in peel geometry. In contrast to both shear and peel loadings, the RSW samples achieved higher energy absorption in X-tension than both sets of SPR joints, although the data had a greater variation. These results suggest that the loading condition has a significant effect on energy absorption behaviour for both processes.



**Figure 11: Energy absorption data at maximum load for SPR and RSW samples – (3+3) stack**

Reviewing the energy absorption results at maximum load,

- RSW in some instances matched or even slightly exceeded the energy absorption performance of SPR joints. However, this depended on the parameters and loading conditions.
- SPR joints generally absorbed more energy under lap shear and peel loading, but RSW joints tended to perform better in X-tension.

A further consideration is the energy absorption at fracture, which can appear to differentiate the two joining processes. An example of energy absorption traces for (1+1) stacks is shown in Figure 12. It can be seen that the tensile extension value for a SPR sample is significantly greater compared to that for an RSW joint. During the riveting process the rivet and the riveted sheets undergo massive deformation to form the mechanical interlock. This energy is stored within the interlock leading to higher energy absorption than that of a fusion formed RSW joint. The nature of the SPR joint/interlock also means that the load can often be sustained significantly longer than a comparable RSW joint, even after the point where the maximum load has been reached.

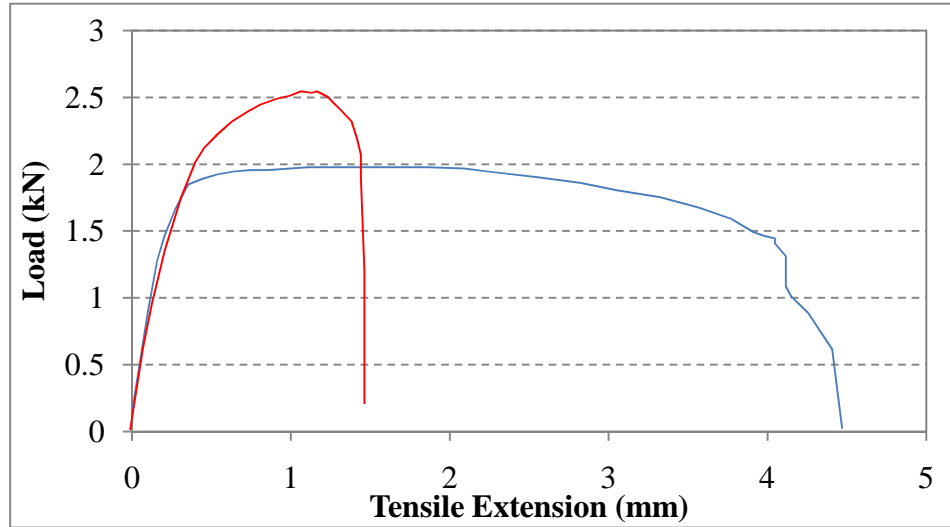


**Figure 12: Energy absorption traces during lap shear test – (1+1) stack**

### 3.6. Asymmetrical stacks – strength comparison

Before discussing the results obtained for the asymmetrical stacks, it is worth highlighting some of the considerations for each process with respect to asymmetry.

For RSW of aluminium, the advantages of the Medium Frequency D.C process are well recognised [19]. However, the directionality of the DC current means more heat is generated at the anode compared to the cathode (due to the thermo-electric Peltier effect). This enhanced heating can sometimes be used to advantage. For example, in an asymmetric stack, the thickest sheet can be oriented to the anode. This would be indicated by the nomenclature (2+1). Comparison with the opposing situation, where the thinner gauge is oriented to the anode, would have the nomenclature (1+2).

For SPR joints the situation is different. As a mechanical joining process, the strength of a SPR joint relies on its interlock. The greater the interlock the higher the joint strength expected. As the interlock is related to the thickness of the locked / bottom sheet, the thinner the bottom layer then usually the smaller the interlock that can be expected, and the greater the risk of breakthrough. The nomenclatures for SPR are (2+1) thickest sheet on top and (1+2) thinnest sheet on top. The effect of this asymmetry for SPR is compared alongside the results for RSW.

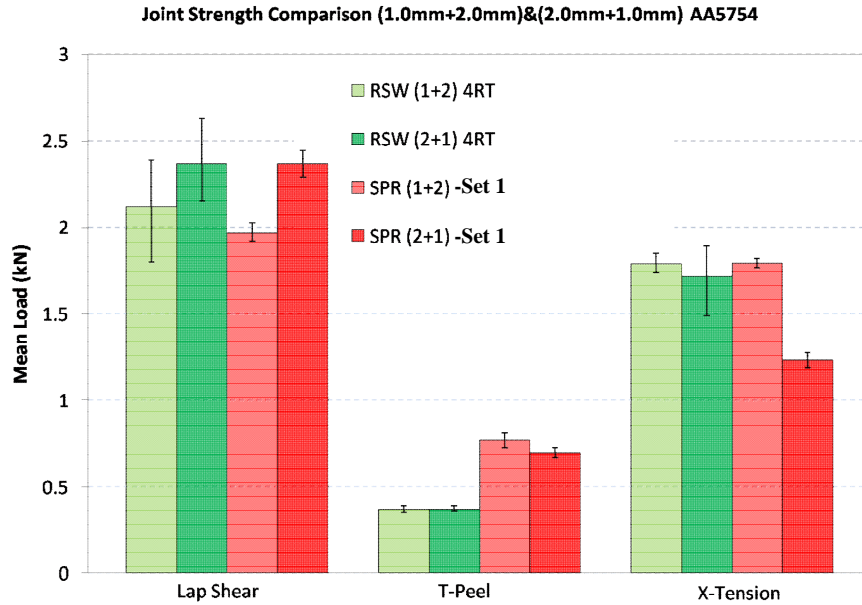
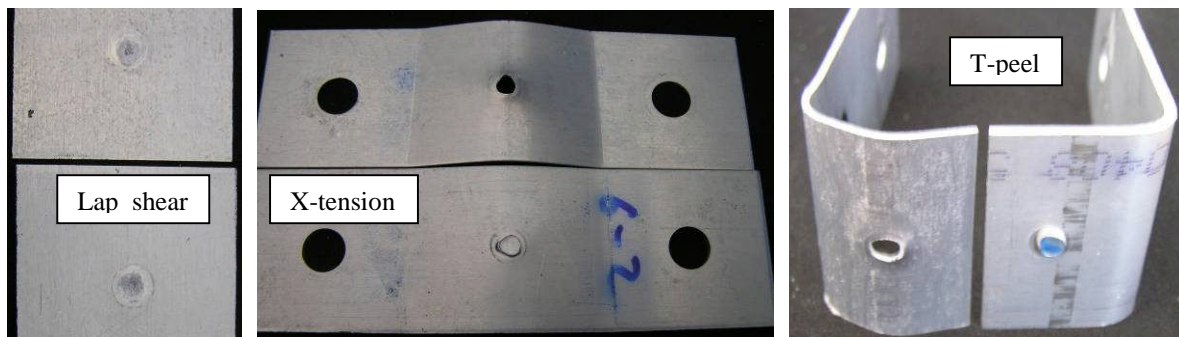


**Figure 13: Joint strength comparison for – (1+2)/(2+1) stacks**

Figure 13 shows the strength test results of (1+2) and (2+1) asymmetrical stacks for both processes. For RSW samples there was no significant effect observed between opposing stacks (1+2) and (2+1) in any of the geometries tested (taking into account the scatter in results shown by the error bars). Both lap shear sample groups failed by nugget/interfacial failure, as shown in Figure 14(a). All T-peel and X-tension samples failed by the thinner sheet material being pulled away from the weld nugget leaving a ‘plug’ of material joined to the thicker sheet, as shown in Figures 14(b) and (c). It follows that for an asymmetric stack that the thinnest sheet will be the governing metal thickness with respect to the strength values that can be expected. Despite the asymmetry of the samples the failure modes observed were the same as for the symmetrical stacks described earlier.



(a) Nugget failure

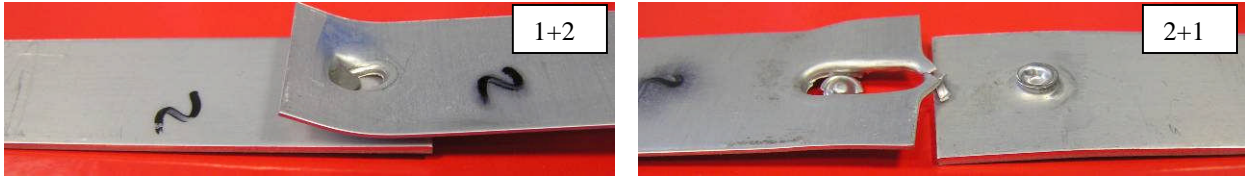
(b) sheet pull-out

(c) sheet pull-out

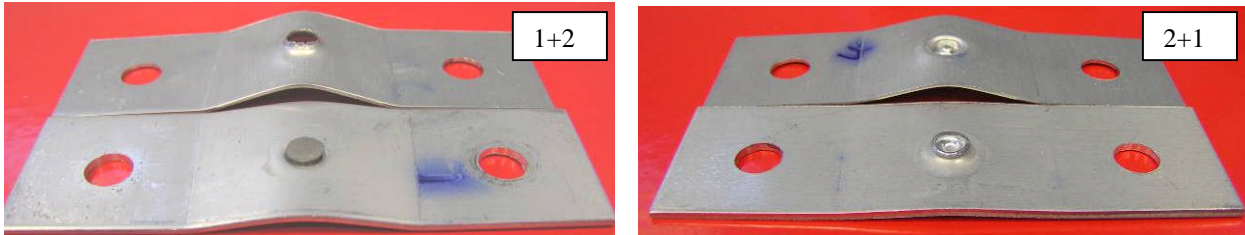
**Figure 14: RSW failure modes for - (1+2)/(2+1) stacks**

For SPR the (2+1) stack exhibited higher shear strength than the (1+2) stack; but lower strength under peel and X-tension loadings. This is attributed to features of the SPR joints and different loading conditions. Under shear loading, the (1+2) stack failed by partial pull-out of the rivet leading to a small degree of tilting; and partial tearing of the top 1.0mm sheet. In contrast, complete tearing of the 1.0mm sheet led to failure of the (2+1) stack leaving the rivet and the 2.0mm top layer untouched. This

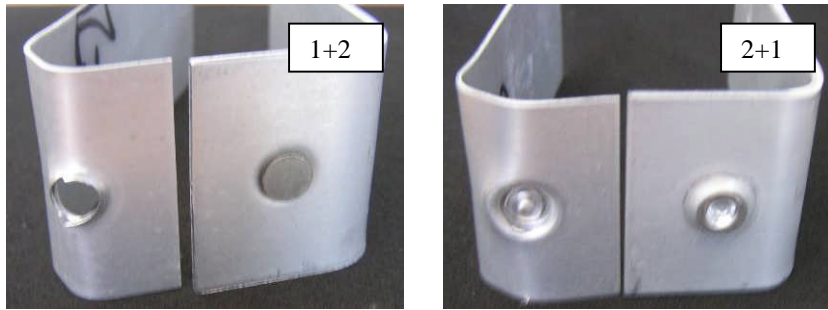
contributed to the higher shear strength of the (2+1) stack and is in agreement with the previous work [14, 20]. In X-tension loading, the interlock strength of the (1+2) stack was sufficient for the rivet head to be pulled through the top 1.0 mm sheet, leading to sheet material failure. In contrast, the (2+1) stack failed by the rivet pull-out the bottom sheet due to a weaker interlock compared with the (1+2) stack, as shown in Figure 15 (b). Similarly these two failure modes that are directly related to the stack and interlock strength, were repeated for the joints tested under T-peel loading, as shown in Figure 15 (c). The results suggest a noticeable effect of stack orientation on SPR joint strength. It is generally advantageous for the thickest sheet in an asymmetric stack to be the bottom sheet, in order to achieve the highest interlock strength.



a) Failure modes for shear test



b) Failure modes for X-tension test



c) Failure mode for T-peel test

**Figure 15: SPR failure modes for – (1+2)/(2+1) stacks**

Results for the thicker asymmetric stacks (2+3) and (3+2) are shown in Figure 16.

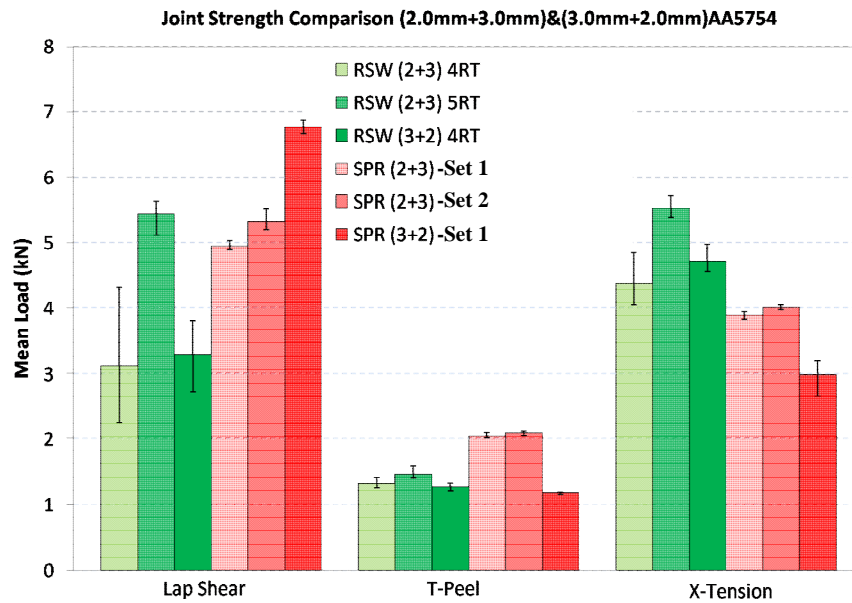
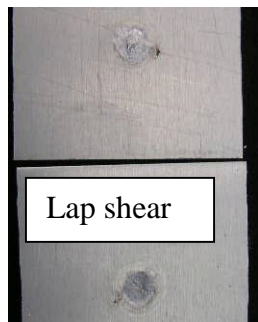
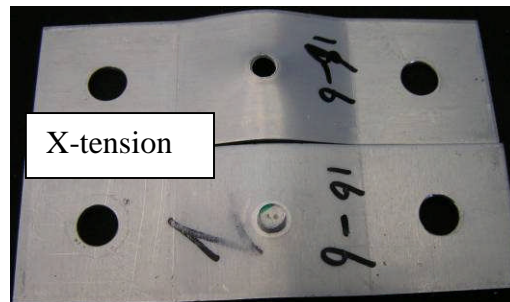


**Figure 16: Joint strength comparison for – (2+3)/ (3+2) stacks**

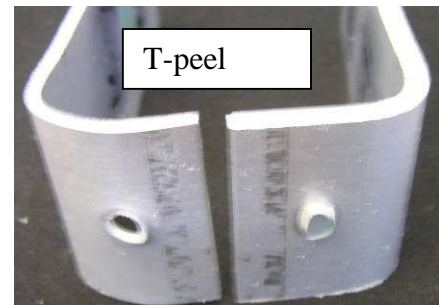
The RSW results show an increase in strength with respect to  $(4\sqrt{t})$  and  $(5\sqrt{t})$  nugget diameters for both lap shear and X-tension geometries; but only a marginal difference for the T-peel geometry. The scatter in results for the (2+3)/(3+2) with smaller  $(4\sqrt{t})$  diameters means that any effect of the stack orientation to the anode electrode is not resolvable. Failure modes for both (2+3) and (3+2) stacks were the same, as shown in Figure 17 using the (2+3) as an example. These failure modes are the same as for the thinner asymmetrical stacks as shown in Figure 14, and were described earlier.



(a) Nugget failure



(b) Sheet pull-out



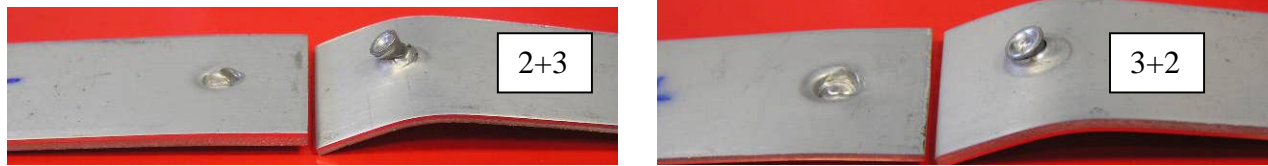
(c) sheet pull-out

**Figure 17: RSW failure modes for – (2+3)/(3+2) stacks**

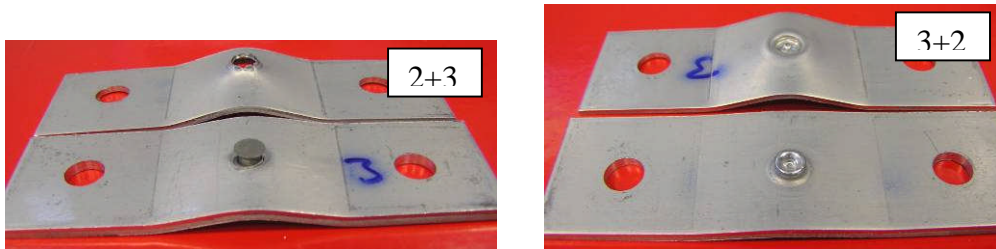
The strength results for the SPR asymmetrical (2+3) and (3+2) stacks generally show the same trends as those observed for the (1+2) and (2+1) thinner gauges (but at approximately twice the strength). Similarly the failure modes under X-tension and T-peel loadings, for both thick and thin sets of asymmetry samples also followed the same trends. The stack orientation effect on SPR joint strength was still obvious. The explanations given earlier for the thinner asymmetrical gauges are equally applicable to the thicker samples shown in Figure 18. However, in contrast to the thin gauge asymmetrical stacks, only rivet pull-out failure was observed for the thick gauge asymmetrical samples



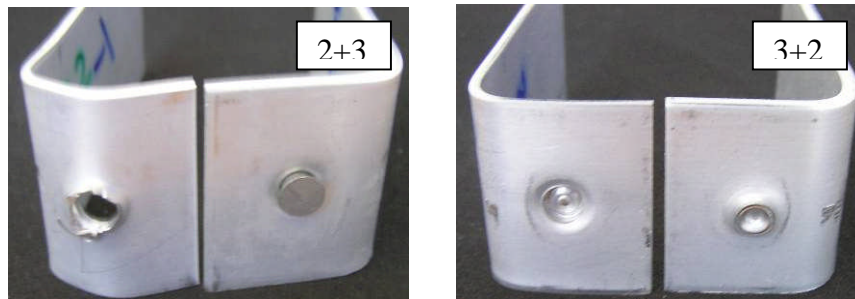
under shear loading. This is because the sheet was thick enough with sufficient strength to prevent being torn, pulled out or peeled away from the rivet head.



a): Failure modes for shear test



b): Failure modes for X-tension test



c): Failure mode for T-peel test

**Figure 18: SPR failure modes for – (2+3)/(3+2) stacks**

### 3.7. Asymmetrical stacks – energy absorption comparison

Figure 19 shows energy absorption data at maximum load for (1+2) and (2+1) stacks. The two sets of RSW samples exhibited similar data, indicating that there was no significant effect of stack orientation. In contrast, for SPR samples, the (2+1) stack had higher energy absorption under shear condition, but lower under peel and X-tension loadings, compared with (1+2) stack. These results followed the same trend as the strength data and suggested a significant effect of stack orientation on energy absorption for SPR joints.

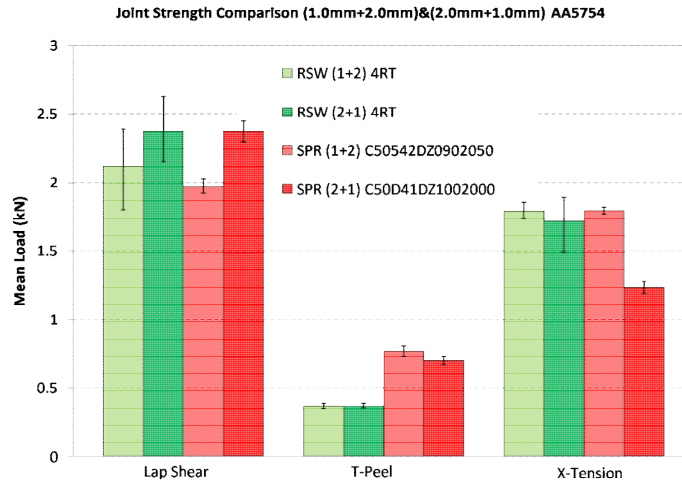


**Figure 19: Energy absorption data at maximum load for SPR and RSW samples – (1+2)/(2+1) stacks**

The energy absorption data for (2+3) and (3+2) stacks are shown in Figure 20. RSW samples with  $5\sqrt{t}$  nugget diameter achieved the highest energy absorption in all three groups of RSW joints indicating the effect of nugget diameter on energy absorption. For SPR joints a same trend as for the (1+2)/(2+1) stacks was observed. This again suggested the effect of stack orientation on energy absorption of a SPR joint.

As discussed earlier, the interlock feature of a SPR joint provides the possibility of achieving higher energy absorption in comparison with a fusion RSW joint. The interlock feature also leads to a significant stack orientation effect on both strength value and energy absorption. Depending on process parameters and loading conditions, RSW samples could achieve similar or even higher energy absorption at maximum load. The stack orientation effect is not obvious.

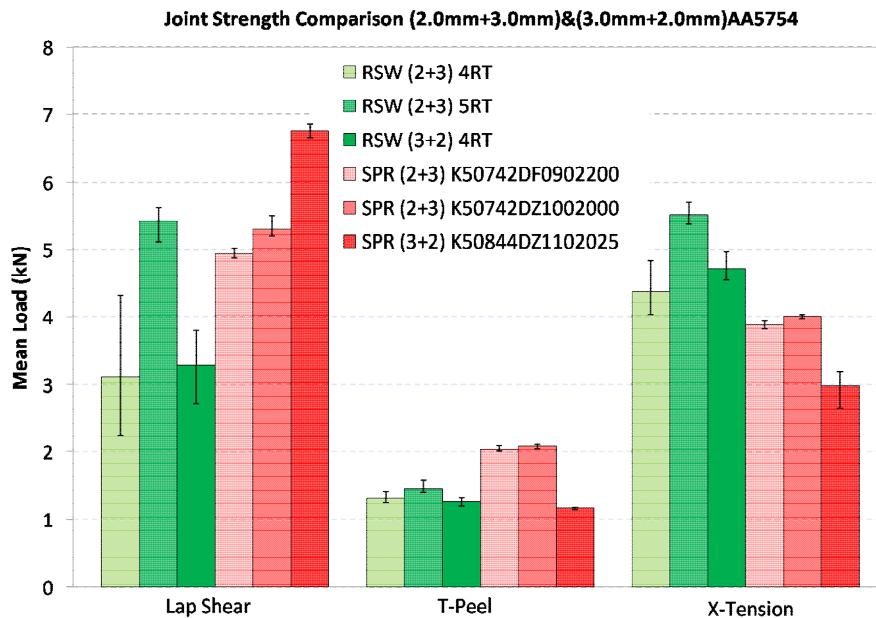


**Figure 20: Energy absorption data at maximum load for SPR and RSW samples – (2+3)/(3+2) stacks**

#### **4. Conclusions**

In comparing SPR and RSW processes it is clear that direct ‘back to back’ analysis is complicated and that often there is not a definitive answer. The nature of the two technologies, one mechanical, the other fusion, means the interaction between their various attributes with the loading geometries tested are important. In addition, the ranking of results can be significantly altered depending on the degree of optimisation of parameters for each process. These points probably account for many of the contradictions in published results, alluded to earlier in the introduction. Despite these difficulties a number of fundamental conclusions can be drawn from the results reported here.

- The selection of process parameters for both RSW and SPR joints affect their strength, energy absorption and failure mode.
- Correlations exist between increasing nugget diameter and strength for lap shear and X-tension loading geometries for RSW joints.
- A general observation is that SPR samples tend to exhibit less scatter than the RSW joints, and the performance of SPR joints improves as the thickness increases.
- SPR joints generally achieved similar or higher peel strengths than the RSW samples.
- For both RSW and SPR technologies: the T-peel joint geometry combined with peel loading provides the lowest strength performance of the three geometries tested.
- For the X-tension test geometry the RSW joint strengths generally match or exceed those for the SPR samples.
- For SPR joints the cross tension test purely tests the interlock of the joints; whilst for RSW samples the periphery of the nugget is tested.
- Stack orientation has no obvious effect on joint strength and energy absorption for RSW samples, but a significant effect for SPR joints.

#### **Acknowledgment**

The authors wish to thank the development agency of Advantage West Midlands, Jaguar Land Rover, Novelis for their support throughout this project.

#### **References**

1. Polmear IJ, “Light alloys”, Third edition, Edward Arnold, 1995.
2. Leitermann W and Christlein J, “The 2<sup>nd</sup> generation Audi space frame of the A2: A trendsetting all-aluminium car body concept in a compact class car”, Seoul 2000 FISITA World automotive congress, June 12-15, 2000, Seoul, Korea.
3. Komatsu Y, Ban K, Ito T, Muraok Y, Yahabo T, Yasunaga K and Shlokawa M, “Application of all aluminium automotive body for Honda NSX”, SAE 910548 (1991).
4. Leone GL and Altshuller B, “Improvement on the resistance spot weldability of aluminium body sheet”, SAE 840292, (1984).
5. Boomer DR, Hunter JA, Castle DR, “A new approach for robust high productivity resistance spot welding of aluminium”, SAE 2003-01-0575, (2003).

6. Spinella DJ, Brockenbrough JR. & Fridy JM “Trends in aluminium resistance spot welding for the auto industry”, *Welding Journal* January 2005 34-40, (2005).
7. Briskham P, Han L, Blundell N, Young K, Hewitt R and Boomer D, “Comparison of self-pierce riveting, resistance spot welding and spot friction joining for aluminium automotive sheet”, SAE 2006 congress, Technical paper, 2006 – 01- 0774, (2006).
8. Briskham P, Boomer D and Hewitt R, “Developments towards high-volume resistance spot welding of aluminium automotive sheet component”, *Lean Weight Vehicle Conference*, (2005).
9. Lapensee M, “No hole riveting”, *Business News Publishing Company*, May 2000.
10. Razmjoo GR and Westgate SA, “Fatigue properties of clinched, self-piercing riveted and spot welded joints in steel and aluminium alloy sheet”, *TWI Report*, 680/1999.
11. Miller KW, Chao YJ and Wang PC, “Performance Comparison of Spot-Welded, Adhesive Bonded, and Self-Piercing Riveted Aluminum Joints”, *ASM Proceedings of the International Conference: Trends in Welding Research*, 1998, p910-915.
12. Riches ST, Westgate SA, Nicholas ED and Powell HJ, “Advanced joining technologies for lightweight vehicle manufacture”, *Materials for low weight vehicles*, 24-25 November, 1995, UK.
13. Westgate SA and Razmjoo GR, “Static and fatigue performance of mechanically fastened and hybrid joints in sheet metals”, *TWI Report*, 691/1999, (1999).
14. Han L, Chrysanthou A and Young K, “Mechanical behaviour of self-piercing riveted multi-layer joints under different specimen configurations”, *Materials & Design* Volume 28, Issue 7, 2007, Pages 2024-2033, (2007).
15. Li Z, Hao C, Zhang J and Zhang H, “Effects of Sheet Surface Conditions on Electrode Life in Resistance Welding Aluminum”, *WELDING JOURNAL*, APRIL 2007
16. Thornton MC, Newton CJ, Keay BFP, Sheasby PG. and Evans JT, “Some surface factors that affect the spot welding of aluminium”, *Trans IMF* 75(4): 165–170, 1997.
17. Crinon E and Evans JT, “The effect of surface roughness, oxide film thickness and interfacial sliding on the electrical contact resistance of aluminium”, *Materials Science and Engineering A*, 242 (1998) 121-128.
18. Ronnhult T, Rilby U and Olefjord I, “The surface state and weldability of aluminium alloys”, *Material science and engineering*, 42 (1980) 329-336.
19. Newton CJ, Boomer DR, Thornton MC and Keay BFP, “The use of medium frequency welding equipment in the resistant spot welding of aluminium automotive sheet”, *Proc. Of “Materials for lean weight vehicle”*, IMC Warwick, UK, 27-28 Nov. 1995.
20. Han L, Young K, Hewitt R and Chrysanthou A, “Effect of breakthrough on the behaviour of self-piercing riveted aluminium 5754 – HSLA joints”, *Transactions of Society of Automotive Engineers of Japan*, Vol.36 No.5 pp181-186, 2005.